Unified Hydrodynamics and Pseudorapidity Distributions of Charged Particles Produced in Heavy Ion Collisions at Low Energies at RHIC *

Zhi-Jin Jiang(姜志进)**, Jia-Qi Hui(惠加琪), Hai-Ping Deng(邓海平)
College of Science, University of Shanghai for Science and Technology, Shanghai 200093

(Received 22 January 2017)

In the context of unified hydrodynamics, we discuss the pseudorapidity distributions of the charged particles produced in Au-Au and Cu-Cu collisions at the low RHIC energies of $\sqrt{s_{\rm NN}} = 19.6$ and 22.4 GeV, respectively. It is found that the unified hydrodynamics alone can give a good description to the experimental measurements. This is different from the collisions at the maximum RHIC energy of $\sqrt{s_{\rm NN}} = 200$ GeV or at LHC energy of $\sqrt{s_{\rm NN}} = 2.76$ TeV, in which the leading particles must be taken into account so that we can properly explain the experimental observations.

PACS: 25.75.Ag, 25.75.Ld, 25.75.−q, 24.10.Nz

DOI: 10.1088/0256-307X/34/5/052501

In the past decade, a number of bulk observables about charged particles, such as the Fourier coefficients v_n of azimuth-angle distributions,[1,2] transverse momentum spectra[3,4] and pseudorapidity distributions,[5–7] have experienced a series of extensive investigations in heavy ion collisions at RHIC and LHC energies. These investigations have provided compelling evidence that the matter created in heavy ion collisions exhibits a clear collective behavior, expanding nearly like an ideal liquid with very low viscosity. This sets up the prominent position of relativistic hydrodynamics in analyzing the properties of bulk observables in heavy ion collisions.[8–26]

In this Letter, the unified hydrodynamics[8] is employed to analyze the pseudorapidity distributions of charged particles produced in heavy ion collisions. The key ingredients of this model are as follows: (1) the expansion of the fluid follows the continuity equation

$$\frac{\partial T^{\mu\nu}}{\partial x^\nu} = 0, \quad \mu,\nu = 0,1, \tag{1}$$

where $x^\nu = (x^0, x^1) = (t, z)$, t is the time, z is the longitudinal coordinate along the beam direction, and $T^{\mu\nu}$ is the energy-momentum tensor. For a perfect fluid, $T^{\mu\nu}$ takes the form as

$$T^{\mu\nu} = (\varepsilon + p)u^\mu u^\nu - p g^{\mu\nu}, \tag{2}$$

where $g^{\mu\nu} = g_{\mu\nu} = \mathrm{diag}(1,-1)$ is the metric tensor, u^μ is the 4-velocity, ε and p are the energy density and pressure of the fluid, respectively, related by

$$\varepsilon = gp, \tag{3}$$

where $1/\sqrt{g} = c_{\rm s}$ is the speed of sound. Plugging Eqs. (2) and (3) into Eq. (1), it becomes

$$\begin{aligned} g\partial_+ \ln p &= -\frac{(g+1)^2}{2}\partial_+ y - \frac{g^2-1}{2}e^{-2y}\partial_- y, \\ g\partial_- \ln p &= \frac{(g+1)^2}{2}\partial_- y + \frac{g^2-1}{2}e^{2y}\partial_+ y, \end{aligned} \tag{4}$$

where y is the ordinary rapidity of fluid, ∂_+ and ∂_- are the partial derivatives with respect to the light-cone coordinates

$$z_\pm = t \pm z = x_0 \pm x_1 = \tau e^{\pm\eta_{\rm S}}, \tag{5}$$

where $\tau = \sqrt{z_+ z_-}$ is the proper time, and $\eta_{\rm S} = 1/2\ln(z_+/z_-)$ is the space-time rapidity.

(2) To solve Eq. (4), the relation between y and $\eta_{\rm S}$ is generalized to the form[8]

$$2y = \ln u_+ - \ln u_- = \ln F_+(z_+) - \ln F_-(z_-), \tag{6}$$

where $u_\pm = u_0 \pm u_1 = e^{\pm y}$ are the light-cone components of 4-velocity, and $F_\pm(z_\pm)$ are the two arbitrary functions. In the case of

$$F_\pm(z_\pm) = z_\pm, \tag{7}$$

Eq. (6) reduces to $y = \eta_{\rm S}$, returning to the boost-invariant picture of Hwa–Bjorken. Otherwise, Eq. (6) describes the non-boost-invariant geometry of Landau. Accordingly, Eq. (6) unifies the Landau with the Hwa–Bjorken hydrodynamics. It plays the role of a bridge between these two models.

By using Eq. (6), Eq. (4) reads as

$$\begin{aligned} g\partial_+ \ln p &= -\frac{(g+1)^2}{4}\frac{f'_+}{f_+} + \frac{g^2-1}{4}\frac{f'_-}{f_+}, \\ g\partial_- \ln p &= -\frac{(g+1)^2}{4}\frac{f'_-}{f_-} + \frac{g^2-1}{4}\frac{f'_+}{f_-}, \end{aligned} \tag{8}$$

where the prime stands for the derivatives with respect to z_+ or z_-, $f_\pm = F_\pm/H$ with H being an arbitrary constant. The solution to Eq. (8) is[8]

$$\begin{aligned} s(z_+, z_-) &= s_0\left(\frac{p}{p_0}\right)^{\frac{g}{g+1}} \\ &= s_0 \exp\left[-\frac{g+1}{4}(l_+^2 + l_-^2) + \frac{g-1}{2}l_+ l_-\right], \end{aligned} \tag{9}$$

*Supported by the Shanghai Key Lab of Modern Optical System.
**Corresponding author. Email: jzj265@163.com

where s is the entropy density of the fluid, s_0 is its initial scale, and

$$l_{\pm}(z_{\pm}) = \sqrt{\ln f_{\pm}}, \quad y(z_+, z_-) = \frac{1}{2}(l_+^2 - l_-^2),$$
$$z_{\pm} = 2h \int_0^{l_{\pm}} e^{u^2} du, \tag{10}$$

where $h = H/A$ with A being an arbitrary constant meeting condition. In this study

$$F_{\pm} F''_{\pm} = \frac{A^2}{2}, \tag{11}$$

where the double prime represents the second derivatives with respect to z_+ or z_-. As $A = 0$, the above equation reduces to $F''_{\pm} = 0$, which gives the solution of $F_{\pm}(z_{\pm}) = z_{\pm} + c$, returning to the Hwa–Bjorken case of Eq. (7) up to a constant c. Hence, the values of A or $h = H/A$ describe the deviation of the system from Hwa–Bjorken expansions. The specific values of h are determined here by comparing the theoretical predictions with experimental data.

(3) As the expansion of the fluid lasts to the time of $t_{\rm FO}$, the inelastic interactions between the particles in the fluid cease, and the abundance of an identified kind of charged particles maintains unchanged. At this moment, the collective motion of the fluid comes to an end, and the fluid decouples or freezes out into the detected particles from a space-like hypersurface with a fixed time of $t_{\rm FO}$. The rapidity distributions of the charged particles frozen out from this hypersurface take the form

$$\frac{dN}{dy} = CN_{\rm Part} e^{-(g-1)(l_+ - l_-)^2/4} \cdot \frac{\partial_+\varphi e^y + \partial_-\varphi e^{-y}}{\partial_+\varphi l_- e^y + \partial_-\varphi l_+ e^{-y}}\Big|_{t_{\rm FO}}, \tag{12}$$

where C is a constant determined here by tuning the theoretical results with the experimental data, and $N_{\rm Part}$ is the number of participants that can be well determined by the Glauber model,[5,27] adopted here to take into account the dependence of distributions on collision centralities. The factor φ in Eq. (12) stands for an arbitrary space-like hypersurface with the time equaling $t_{\rm FO}$, which can be taken as

$$\varphi(z_+, z_-) = t_{\rm FO} = \frac{1}{2}(z_+ + z_-). \tag{13}$$

Substituting Eq. (13) into Eq. (12), we have

$$\frac{dN}{dy} = CN_{\rm Part} \frac{e^{-(g-1)(l_+ - l_-)^2/4}}{l_- + l_+ + (l_- - l_+)\tanh y}. \tag{14}$$

With the above equation, the pseudorapidity distribution of charged particles measured in experiments can be expressed as

$$\frac{dN}{d\eta} = \sqrt{1 - \frac{m^2}{m_{\rm T}^2 \cosh^2 y}}\, \frac{dN}{dy}, \tag{15}$$

with

$$y = \frac{1}{2} \ln \left[\frac{\sqrt{p_{\rm T}^2 \cosh^2 \eta + m^2} + p_{\rm T} \sinh \eta}{\sqrt{p_{\rm T}^2 \cosh^2 \eta + m^2} - p_{\rm T} \sinh \eta} \right], \tag{16}$$

where $p_{\rm T}$ is the transverse momentum, and $m_{\rm T} = \sqrt{m^2 + p_{\rm T}^2}$ is the transverse mass.

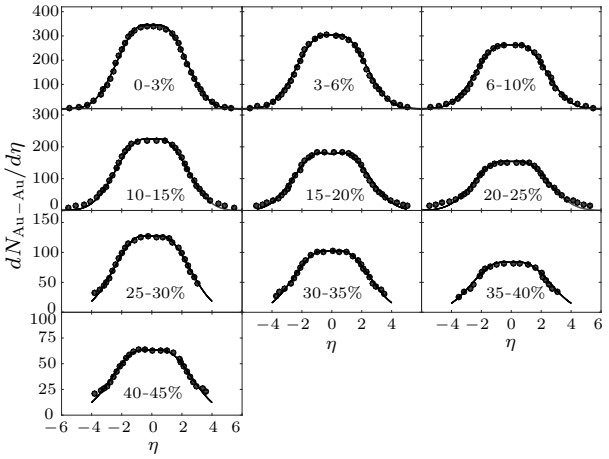

Fig. 1. The pseudorapidity distributions of produced charged particles in different centrality Au-Au collisions at $\sqrt{s_{\rm NN}} = 19.6$ GeV. The solid dots are the experimental measurements.[5] The solid curves are the results from the unified hydrodynamics of Eq. (15).

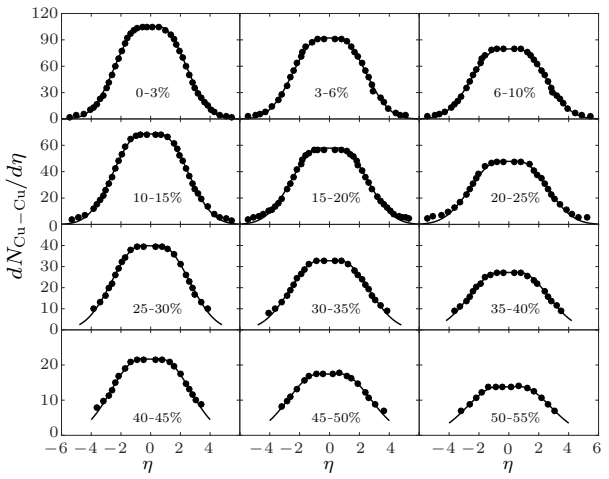

Fig. 2. The pseudorapidity distributions of produced charged particles in different centrality Cu-Cu collisions at $\sqrt{s_{\rm NN}} = 22.4$ GeV. The solid dots are the experimental measurements.[5] The solid curves are the results from unified hydrodynamics of Eq. (15).

Inserting Eq. (14) into Eq. (15), we can obtain the pseudorapidity distributions of the charged particles. The results are shown in Figs. 1 and 2, which are for different centrality Au-Au and Cu-Cu collisions at $\sqrt{s_{\rm NN}} = 19.6$ and 22.4 GeV, respectively. The solid dots in the figures are the experimental measurements.[5] The solid curves are the results from Eq. (15).

Investigations have shown that the speed of sound related factor g in Eq. (3) decreases slowly with incre-

asing the collision energy. For a given incident energy, g changes very slowly with collision systems and centrality cuts.[28–31] In Ref. [28], g takes the value of $g = 8.16$ for Au-Au collisions at $\sqrt{s_{\rm NN}} = 200\,{\rm GeV}$. Conferring this, g takes approximately the values of $g = 8.7$ and 8.5 in the calculations for Au-Au and Cu-Cu collisions, respectively.

The parameter h in Eq. (10) takes the values as those summarized in Table 1. It can be seen that h decreases with increasing energies and centrality cuts. It should vary in this way, since the larger the energy and centrality cut are, the more transparent the nucleus becomes; the produced charged particles will then be located in a broader rapidity region. However, the region of rapidity distributions of Eq. (14) is mainly determined by h. The broader the region of rapidity distributions is, the smaller the value of h is. This can be seen in Fig. 3, which is for Au-Au collisions normalized to 0–3% centrality cut. The narrower curve is the corresponding rapidity distribution in Fig. 1, obtained by using $h = 0.14$. The broader one is for $h = 0.0014$. Hence, the region of rapidity distributions increases with decreasing h. This forms the basis for the above fitted h values.

Table 1. The value of h, the number of participants $N_{\rm Part}$ and the parameter C in different centrality Au-Au and Cu-Cu collisions.

Centrality cuts (%)	h		$N_{\rm Part}$		C	
	Au-Au (10^{-3})	Cu-Cu (10^{-4})	Au-Au	Cu-Cu	Au-Au	Cu-Cu
0–3	140.0	450.0	351 ± 11	103 ± 3	7.81	8.45
3–6	85.0	250.0	322 ± 10	95 ± 3	7.63	8.20
6–10	53.0	100.0	286 ± 9	86 ± 3	7.58	8.06
10–15	45.0	85.0	247 ± 8	74 ± 3	7.52	8.12
15–20	15.0	45.0	206 ± 8	63 ± 3	7.79	8.21
20–25	8.2	30.0	171 ± 7	53 ± 3	7.91	8.17
25–30	7.1	20.0	142 ± 7	44 ± 3	7.92	8.30
30–35	4.5	10.0	117 ± 7	37 ± 3	7.80	8.27
35–40	1.5	8.5	95 ± 7	30 ± 3	8.11	8.50
40–45	0.8	6.5	74 ± 6	25 ± 3	8.01	8.20
45–50	–	1.5	–	20 ± 3	–	8.55
50–55	–	0.9	–	16 ± 3	–	8.56

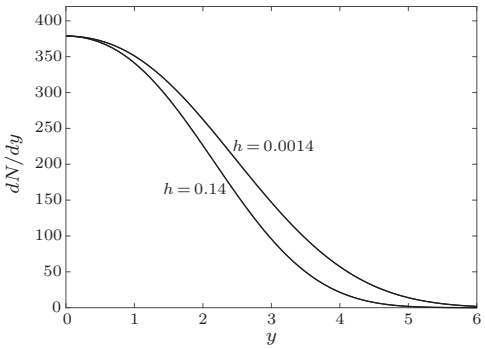

Fig. 3. The rapidity distributions of produced charged particles for two different values of h in Au-Au collisions normalized to 0–3% centrality cut.

Table 1 also lists the fitted constant C together with the number of participants[5] $N_{\rm Part}$ in Eq. (12) in both collision situations in different centrality cuts. It can be seen that, for a given incident energy and collision system, C almost maintains unchanged to a certain extent. This means that, just as the assumptions made above, the centrality dependence of dN/dy is largely determined by $N_{\rm Part}$.

Figures 1 and 2 show that the unified hydrodynamics alone can give a good description to the pseudorapidity distributions of charged particles measured in nucleus-nucleus collisions at low energies at RHIC. This is unlike the situations in collisions at the maximum RHIC energy of $\sqrt{s_{\rm NN}} = 200\,{\rm GeV}$ or at LHC energy of $\sqrt{s_{\rm NN}} = 2.76\,{\rm TeV}$, where the leading particles are essential in explaining experimental measurements.[19] This difference may arise from the transparency of participants in different incident energies.[32]

In conclusion, the hot and dense matter created in heavy ion collisions is assumed to evolve according to the relativistic hydrodynamics, which integrates the characteristics of Landau and the Hwa–Bjorken hydrodynamics by generalizing the relation between ordinary rapidity y and space-time rapidity $\eta_{\rm S}$. This is one of a very few hydrodynamic models which can be solved analytically. The solutions can then be utilized to formulate the rapidity distributions of charged particles frozen out from a space-like hypersurface with a fixed time of $t_{\rm FO}$. In the derived formula, there are three parameters: g, C and h. Known from comparing with experimental measurements, g and C almost maintain unchanged for different centrality cuts, while h decreases with increasing the centrality cut. Compared with the pseudorapidity distributions of the charged particles measured by RHIC-PHOBOS collaboration in Au-Au and Cu-Cu collisions at respective energies of $\sqrt{s_{\rm NN}} = 19.6$ and 22.4 GeV, we can see that the results from unified hydrodynamics match up well with the experimental data.

References

[1] Adamczyk L et al 2016 *Phys. Rev.* C **93** 014907
[2] Adam J et al 2016 *Phys. Rev. Lett.* **116** 132302
[3] Chatrchyan S et al 2012 *Eur. Phys. J.* C **72** 2164
[4] Abelev B et al 2013 *Phys. Rev.* C **88** 044910
[5] Alver B et al 2011 *Phys. Rev.* C **83** 024913
[6] Abbas E et al 2013 *Phys. Lett.* B **726** 610
[7] Bearden I G et al 2005 *Phys. Rev. Lett.* **94** 162301
[8] Bialas A, Janik R A and Peschanski R 2007 *Phys. Rev.* C

76 054901
[9] Bialas A and Peschanski R 2011 *Phys. Rev.* C **83** 054905
[10] Suzuki N 2010 *Phys. Rev.* C **81** 044911
[11] Sarkisyan E K G, Mishra A N, Sahoo R and Sakharov A S 2016 *Phys. Rev.* D **93** 054046
[12] Sarkisyan E K G, Mishra A N, Sahoo R and Sakharov A S 2016 *Phys. Rev.* D **94** 011501
[13] Gale C, Jeon S and Schenke B 2013 *Physica* A **28** 1340011
[14] Heinz U and Snellings R 2013 *Annu. Rev. Nucl. Part. Sci.* **63** 123
[15] Beuf G, Peschanski R and Saridakis E N 2008 *Phys. Rev.* C **78** 064909
[16] Wong C Y 2008 *Phys. Rev.* C **78** 054902
[17] Sarkisyan E K G and Sakharov A S 2010 *Eur. Phys. J.* C **70** 533
[18] Mishra A N, Sahoo R, Sarkisyan E K G and Sakharov A S 2014 *Eur. Phys. J.* C **74** 3147
[19] Jiang Z J, Deng H P and Zhang Y 2016 *Adv. High Ener Phys.* **2016** 5308084
[20] Wang Z W, Jiang Z J and Zhang Y S 2009 *J. Univ. Shanghai Sci. Technol.* **31** 322 (in Chinese)
[21] Jiang Z J, Li Q G and Zhang H L 2013 *Phys. Rev.* C **87** 044902
[22] Zhang H L, Jiang Z J and Jiang G X 2014 *Chin. Phys. Lett.* **31** 022501
[23] Jiang Z J, Zhang Y, Zhang H L and Deng H P 2015 *Nucl. Phys.* A **941** 188
[24] CsörgőT, Nagy M I and Csanád M 2008 *Phys. Lett.* B **663** 306
[25] Csanád M, Nagy M I and Lökö S 2012 *Eur. Phys. J.* A **48** 173
[26] Noronha-Hostler J, Luzum M and Ollitrault J Y 2016 *Phys. Rev.* C **93** 034912
[27] Jiang Z J 2007 *Acta Phys. Sin.* **56** 5191 (in Chinese)
[28] Adare A et al 2007 *Phys. Rev. Lett.* **98** 162301
[29] Gao L N, Chen Y H, Wei H R and Liu F H 2013 *Adv. High Energy Phys.* **2014** 450247
[30] Mizoguchi T, Miyazawa H and Biyajima M 2009 *Eur. Phys. J.* A **40** 99
[31] Borsányi S, Endrődi G, Fodor Z, Jakovác A, Katz S D, Krieg S, Ratti C and Szabó K K 2010 *J. High Energy Phys.* **1011** 077
[32] Jiang Z J, Huang Y, Zhang H L and Zhang Y 2017 *Pramana* **88** 63